

IETI-DP for Conforming Multi-Patch Isogeometric Analysis in Three Dimensions

Rainer Schneckleitner

Institute of Computational Mathematics, Johannes Kepler University
Altenberger Str. 69, 4040 Linz, Austria

Stefan Takacs

Johann Radon Institute for Computational and Applied Mathematics
Austrian Academy of Sciences
Altenberger Str. 69, 4040 Linz, Austria

NuMa-Report No. 2021-03

March 2021

Technical Reports before 1998:

1995

- 95-1 Hedwig Brandstetter
Was ist neu in Fortran 90? March 1995
- 95-2 G. Haase, B. Heise, M. Kuhn, U. Langer
Adaptive Domain Decomposition Methods for Finite and Boundary Element Equations. August 1995
- 95-3 Joachim Schöberl
An Automatic Mesh Generator Using Geometric Rules for Two and Three Space Dimensions. August 1995

1996

- 96-1 Ferdinand Kickingger
Automatic Mesh Generation for 3D Objects. February 1996
- 96-2 Mario Goppold, Gundolf Haase, Bodo Heise und Michael Kuhn
Preprocessing in BE/FE Domain Decomposition Methods. February 1996
- 96-3 Bodo Heise
A Mixed Variational Formulation for 3D Magnetostatics and its Finite Element Discretisation. February 1996
- 96-4 Bodo Heise und Michael Jung
Robust Parallel Newton-Multilevel Methods. February 1996
- 96-5 Ferdinand Kickingger
Algebraic Multigrid for Discrete Elliptic Second Order Problems. February 1996
- 96-6 Bodo Heise
A Mixed Variational Formulation for 3D Magnetostatics and its Finite Element Discretisation. May 1996
- 96-7 Michael Kuhn
Benchmarking for Boundary Element Methods. June 1996

1997

- 97-1 Bodo Heise, Michael Kuhn and Ulrich Langer
A Mixed Variational Formulation for 3D Magnetostatics in the Space $H(\text{rot}) \cap H(\text{div})$ February 1997
- 97-2 Joachim Schöberl
Robust Multigrid Preconditioning for Parameter Dependent Problems I: The Stokes-type Case. June 1997
- 97-3 Ferdinand Kickingger, Sergei V. Nepomnyaschikh, Ralf Pfau, Joachim Schöberl
Numerical Estimates of Inequalities in $H^{\frac{1}{2}}$. August 1997
- 97-4 Joachim Schöberl
Programmbeschreibung NAOMI 2D und Algebraic Multigrid. September 1997

From 1998 to 2008 technical reports were published by SFB013. Please see

<http://www.sfb013.uni-linz.ac.at/index.php?id=reports>

From 2004 on reports were also published by RICAM. Please see

<http://www.ricam.oeaw.ac.at/publications/list/>

For a complete list of NuMa reports see

<http://www.numa.uni-linz.ac.at/Publications/List/>

IETI-DP for conforming multi-patch Isogeometric Analysis in three dimensions

Rainer Schneckleitner and Stefan Takacs*

Abstract We consider dual-primal isogeometric tearing and interconnection (IETI-DP) solvers for multi-patch geometries in Isogeometric Analysis. Recently, the authors have published a convergence analysis for those solvers that is explicit in both the grid size and the spline degree for conforming discretizations of two dimensional computational domains. In the present paper, we shortly revisit these results and provide numerical experiments that indicate that similar results may hold for three dimensional domains.

1 Introduction

We are interested in fast domain decomposition solvers for multi-patch Isogeometric Analysis (IgA; [4]). We focus on variants of FETI-DP solvers, see [2, 10] and references therein. Such methods have been adapted to IgA in [5], where the individual patches of the multi-patch discretization are used as subdomains for the solver. This method is sometimes referred to as the dual-primal isogeometric tearing and interconnection (IETI-DP) method. These methods are similar to Balancing Domain Decomposition by Constraints (BDDC) methods, which have also been adapted for IgA, see [1] and follow-up papers by the same authors. The similarity is outlined in [6].

Rainer Schneckleitner
RICAM, Austrian Academy of Sciences, Altenberger Straße 69, 4040 Linz, Austria e-mail:
`schneckleitner@numa.uni-linz.ac.at`

Stefan Takacs
RICAM, Austrian Academy of Sciences, Altenberger Straße 69, 4040 Linz, Austria e-mail:
`stefan.takacs@ricam.oeaw.ac.at`

* Corresponding Author

Much progress for the IETI-DP methods has been made in the PhD-thesis by C. Hofer, including the extension to various discontinuous Galerkin formulations, see [3]. Recently, the authors of the paper at hand have extended the condition number bounds for the preconditioned Schur complement system to be explicit not only in the grid size but also in the chosen spline degree, see [8] for the conforming case and [9] for an extension to the discontinuous Galerkin case. The analysis follows the framework from [6]. One key ingredient for the analysis in [8] has been the construction of a bounded harmonic extension operator for splines, which followed the ideas of [7]. The analysis in [8] treats the two-dimensional case. As usual for FETI-like methods, the extension of the analysis to three dimensions is not effortless. The goal of this paper is to demonstrate that the proposed method also performs well for higher spline degrees in three dimensions.

The remainder of this paper is organized as follows. In Section 2, we introduce the model problem, discuss its discretization and the proposed IETI-DP algorithm. In Section 3, numerical experiments for a three dimensional example are presented.

2 Model problem and its solution

We consider a standard Poisson model problem. Let $\Omega \subset \mathbb{R}^d$ be a bounded Lipschitz domain. For given $f \in L_2(\Omega)$, we are interested in solving for $u \in H^1(\Omega)$ such that

$$-\Delta u = f \quad \text{in } \Omega \quad \text{and} \quad u = 0 \quad \text{on } \partial\Omega$$

holds in a weak sense. We assume that the closure of the computational domain Ω is the union of the closure of k non-overlapping patches $\Omega^{(k)}$ that are parametrized with geometry functions

$$G_k : \widehat{\Omega} := (0, 1)^d \rightarrow \Omega^{(k)} := G_k(\widehat{\Omega})$$

such that for any $k \neq \ell$, the intersection $\overline{\Omega^{(k)}} \cap \overline{\Omega^{(\ell)}}$ is empty, a common vertex, a common edge, or (in three dimensions) a common face (cf. [8, Ass. 2]). We assume that both, ∇G_k and $(\nabla G_k)^{-1}$, are in $L_\infty(\widehat{\Omega})$ for all patches. For the analysis, we need a uniform bound on the L_∞ -norm and a uniform bound on the number of neighbors of each patch, cf. [8, Ass. 1 and 3].

For each of the patches, we introduce a tensor B-spline discretization on the parameter domain $\widehat{\Omega}$. The discretization is then mapped to the physical patch $\Omega^{(k)}$ using the pull-back principle. We use a standard basis as obtained by the Cox-de Boor formula. We need a fully matching discretization, this means that for each basis function that has a non-vanishing trace on one

of the interfaces, there is exactly one basis function on each of the patches sharing this interface such that the traces of the basis functions agree (cf. [8, Ass. 5]). This is a standard assumption for any multi-patch setting that is not treated using discontinuous Galerkin methods. For the analysis, we assume quasi uniformity of grids within each patch, cf. [8, Ass. 4].

In the following, we explain how the IETI-DP solver is set up. Here, we loosely follow the notation used in the IETI-DP solution framework that recently joined the public part of the G+Smo library. We choose the patches as IETI subdomains. We obtain patch-local stiffness matrices $A^{(k)}$ by evaluating the bilinear forms $a^{(k)}(u, v) = \int_{\Omega^{(k)}} \nabla^\top u(x) \nabla v(x) dx$ with the basis functions for the corresponding patch. We set up matrices $C^{(k)}$ such that their null space are the coefficient vectors of the patch-local functions that vanish at the primal degrees of freedom. In [8], we have considered corner values, edge averages, and the combination of both. In the three dimensional case, we can choose corner values, edge averages, face averages, and any combination thereof. We set up fully redundant jump matrices $B^{(k)}$. We omit the corner values if and only if the corners are chosen as primal degrees of freedom. We setup the primal problem in the usual way, i.e., we first, for $k = 1, \dots, K$, compute a basis by

$$\Psi^{(k)} := (I \ 0) (\tilde{A}^{(k)})^{-1} \begin{pmatrix} 0 \\ R_c^{(k)} \end{pmatrix}, \quad \text{where} \quad \tilde{A}^{(k)} := \begin{pmatrix} A^{(k)} & (C^{(k)})^\top \\ C^{(k)} & \end{pmatrix}$$

and $R_c^{(k)}$ is a binary matrix that relates the primal constraints (with their patch-local indices) to the degrees of freedom of the primal problem (with their global indices) and set then

$$\tilde{A}^{(K+1)} := \sum_{k=1}^K (\Psi^{(k)})^\top A^{(k)} \Psi^{(k)}, \quad \text{and} \quad \tilde{B}^{(K+1)} := \sum_{k=1}^K B^{(k)} \Psi^{(k)}.$$

We consider the Schur complement problem $F \underline{\lambda} = \underline{g}$, where

$$F := \sum_{k=1}^{K+1} \tilde{B}^{(k)} (\tilde{A}^{(k)})^{-1} (\tilde{B}^{(k)})^\top \quad \text{and} \quad \tilde{B}^{(k)} := (B^{(k)} \ 0) \quad \text{for } k = 1, \dots, K.$$

The derivation of \underline{g} is a patch-local preprocessing step. We solve the Schur complement problem using a preconditioned conjugate gradient (PCG) solver with the scaled Dirichlet preconditioner

$$M_{\text{SD}} := \sum_{k=1}^K B_\Gamma D_k^{-1} \left(A_{\Gamma\Gamma}^{(k)} - A_{\Gamma I}^{(k)} (A_{II}^{(k)})^{-1} A_{I\Gamma}^{(k)} \right) D_k^{-1} (B_\Gamma)^\top,$$

where the index Γ refers to the rows/columns of $A^{(k)}$ and the columns of $B^{(k)}$ that refer to basis functions with non-vanishing trace, the index I refers to the remaining rows/columns, and the matrix D_k is a diagonal matrix defined based on the principle of multiplicity scaling. For the analysis, it is important that its coefficients are constant within each interface. The solution u itself is obtained from $\underline{\lambda}$ using the usual patch-local steps, cf. [8].

Under the presented assumptions, the condition number of the preconditioned Schur complement system is in the two-dimensional case bounded by

$$C p \left(1 + \log p + \max_{k=1, \dots, K} \log \frac{H_k}{h_k} \right)^2,$$

where p is the spline degree, H_k is the patch size, and h_k the grid size, see [8].

3 Numerical results

In the following, we present numerical results for a three dimensional domain and refer to the original paper [8] for the two dimensional case. The computational domain Ω is a twisted version of a Fichera corner, see Fig. 1. The original geometry consists of 7 patches. We subdivide each patch uniformly into $4 \times 4 \times 4$ patches to obtain a decomposition into 448 patches.

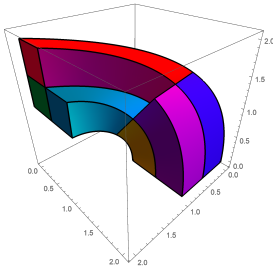


Fig. 1: Computational domain

We solve the model problem $-\Delta u(x, y, z) = 3\pi^2 \sin(\pi x) \sin(\pi y) \sin(\pi z)$ for $(x, y, z) \in \Omega$ with homogeneous Dirichlet boundary conditions on $\partial\Omega$ by means of the IETI-DP solver outlined in the previous sections. Within the patches, we consider tensor-product B-spline discretizations of degree p and maximum smoothness C^{p-1} . We consider several grid sizes, the refinement level $r = 0$ corresponds to a discretization of each patch with polynomials. The next refinement levels $r = 1, 2, \dots$ are obtained by uniform refinement.

All experiments have been carried out in the C++ library G+Smo¹ and have been executed on the Radon1 cluster² in Linz. All computations have been performed with a single core.

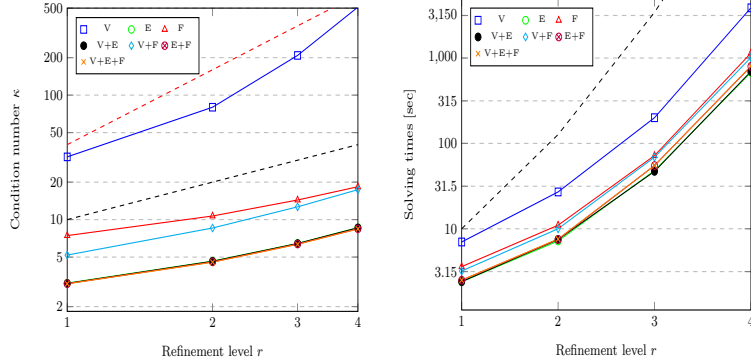


Fig. 2: Condition numbers and solving times for $p = 3$

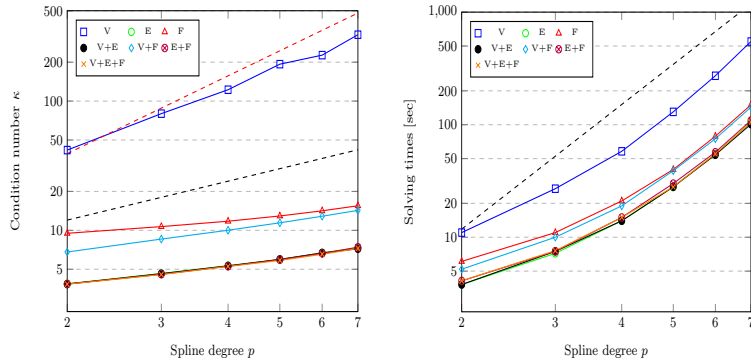


Fig. 3: Condition numbers and solving times for $r = 2$

Concerning the choice of the primal degrees of freedom, we consider all possibilities. For the two-dimensional case, the common choices are the corner values, the edge averages, and a combination of both. We have seen in [8] that all approaches work, typically the corner values better than the edge averages. As expected, the combination of both yields the best results. For the three dimensional case, we have more possibilities. We report on these approaches

¹ <https://github.com/gismo/gismo>, example file `examples/ieti_example.cpp`.

² <https://www.ricam.oeaw.ac.at/hpc/>

r	$p = 2$		$p = 3$		$p = 4$		$p = 5$		$p = 6$		$p = 7$	
	it	κ	it	κ	it	κ	it	κ	it	κ	it	κ
1	33	14	51	32	64	45	89	84	108	109	136	178
2	57	42	79	80	98	122	124	193	148	227	176	326
3	94	116	123	208	149	315	175	439	199	566	OoM	
4	146	275	176	509	OoM		OoM		OoM		OoM	

Table 1: Iterations (it) and condition number (κ); Vertex (V)

r	$p = 2$		$p = 3$		$p = 4$		$p = 5$		$p = 6$		$p = 7$	
	it	κ	it	κ	it	κ	it	κ	it	κ	it	κ
1	14	2.5	17	3.1	20	3.8	23	4.4	27	5.1	29	5.5
2	18	3.9	21	4.6	23	5.3	26	6.0	29	6.7	32	7.3
3	23	5.6	25	6.4	28	7.3	30	8.0	33	8.8	OoM	
4	27	7.5	30	8.6	OoM		OoM		OoM		OoM	

Table 2: Iterations (it) and condition number (κ); Edges (E)

r	$p = 2$		$p = 3$		$p = 4$		$p = 5$		$p = 6$		$p = 7$	
	it	κ	it	κ	it	κ	it	κ	it	κ	it	κ
1	22	6.1	26	7.4	29	8.3	33	9.5	37	10.4	41	11.5
2	29	9.5	31	10.7	34	11.8	37	12.9	42	14.2	46	15.5
3	35	13.1	38	14.4	41	15.9	43	17.0	47	18.3	OoM	
4	41	17.1	44	18.4	OoM		OoM		OoM		OoM	

Table 3: Iterations (it) and condition number (κ); Faces (F)

in the Tables 1 (vertex values = V), 2 (edge averages = E), 3 (face averages = F), 4 (V+E), 5 (V+F), and 6 (E+F). The combination of all variants (V+E+F) is almost identical to the case V+E and only included in the diagrams. In any case, we report on the number of iterations (it) required by the PCG solver to reduce the residual with a random starting vector by a factor of 10^{-6} compared to the right-hand side. Moreover, we report on the condition numbers (κ) of the preconditioned system as estimated by the PCG solver.

In Figure 2, the dependence on the refinement level is depicted. Here, we have chosen the spline degree $p = 3$ and have considered all of the possibilities for primal degrees of freedom. Here, we have 44 965 ($r = 1$), 133 629 ($r = 2$), 549 037 ($r = 3$), and 2 934 285 ($r = 4$) degrees of freedom (dofs). We observe that choosing only vertex values as primal degrees of freedom leads to the largest condition numbers. We observe that in this case the con-

r	$p = 2$		$p = 3$		$p = 4$		$p = 5$		$p = 6$		$p = 7$	
	it	κ	it	κ	it	κ	it	κ	it	κ	it	κ
1	14	2.5	17	3.1	20	3.8	22	4.3	26	5.0	28	5.4
2	18	3.8	21	4.6	23	5.3	26	6.0	29	6.7	31	7.2
3	22	5.5	25	6.4	28	7.3	30	8.0	33	8.8	OoM	
4	27	7.5	30	8.6	OoM		OoM		OoM		OoM	

Table 4: Iterations (it) and condition number (κ); Vertices+Edges (V+E)

r	$p = 2$		$p = 3$		$p = 4$		$p = 5$		$p = 6$		$p = 7$	
	it	κ	it	κ	it	κ	it	κ	it	κ	it	κ
1	17	3.7	22	5.2	26	6.6	30	7.8	34	9.0	38	10.1
2	25	6.8	29	8.6	32	10.0	36	11.4	40	12.9	44	14.3
3	32	10.7	36	12.7	39	14.2	42	15.6	45	17.3	OoM	
4	39	15.2	43	17.4	OoM		OoM		OoM		OoM	

Table 5: Iterations (it) and condition number (κ); Vertices+Face (V+F)

r	$p = 2$		$p = 3$		$p = 4$		$p = 5$		$p = 6$		$p = 7$	
	it	κ	it	κ	it	κ	it	κ	it	κ	it	κ
1	14	2.5	17	3.1	20	3.8	23	4.3	27	5.0	30	5.7
2	19	3.9	21	4.6	24	5.3	27	5.9	30	6.6	33	7.4
3	23	5.5	26	6.4	29	7.2	31	7.9	33	8.5	OoM	
4	28	7.4	31	8.4	OoM		OoM		OoM		OoM	

Table 6: Iterations (it) and condition number (κ); Edges+Faces (E+F)

dition number grows like r^2 (the dashed red line indicates the slope of such a growth). This corresponds to a growth like $(1 + \log H/h)^2$, as predicted by the theory for the two-dimensional case. All other options yield significantly better results, particularly those that include edge averages. In these cases, the growth seems to be less than linear in $r \approx \log H/h$ (the dashed black line shows such a slope). In the right diagram, we can see that choosing a strategy with smaller condition numbers also yields a faster method. Since the dimensions and the bandwidths of the local stiffness matrices grow like $(H_k/h_k)^3$ and $(H_k/h_k)^2$, respectively, the complexity of the LU decompositions grows like $\sum_{k=1}^K (H_k/h_k)^7$. The complexity analysis indicates that they are the dominant factor. The dashed black line indicates such a growth.

In Figure 3, the dependence on the spline degree is presented, where we have chosen $r = 2$. Here, the number of dofs ranges from 66 989 ($p = 2$) to

549037 ($p = 7$). Also in this picture, we see that the vertex values perform worst and the edge averages best. Again, we obtain a different asymptotic behavior for the corner values. For those primal degrees of freedom, the condition number grows like p^2 (the dashed red line indicates the corresponding slope). All the other primal degrees of freedom seem to lead to a growth that is smaller than linear in p (the dashed black line indicates the slope of a linear growth). Note that for the two-dimensional case, the theory predicts a growth like $p(1 + \log p)^2$. In the right diagram, we can see that the solving times grow like p^4 (the dashed line shows the corresponding slope). This seems to be realistic since the number of non-zero entries of the stiffness matrix grows like Np^d , where N is the number of unknowns. For $d = 3$, this yields in combination with the condition number bound the observed rates.

Concluding, in this paper we have seen that the IETI method as described in [8] can indeed be extended to the three dimensional case. As for finite elements, only choosing vertex values is not enough.

Acknowledgements The first author was supported by the Austrian Science Fund (FWF): S117-03 and W1214-04. Also, the second author has received support from the Austrian Science Fund (FWF): P31048.

References

1. L. Beirão da Veiga, D. Cho, L. Pavarino, and S. Scacchi. BDDC preconditioners for isogeometric analysis. *Math. Models Methods Appl. Sci.*, 23(6):1099 – 1142, 2013.
2. C. Farhat, M. Lesoinne, P. L. Tallec, K. Pierson, and D. Rixen. FETI-DP: A dual-primal unified FETI method I: A faster alternative to the two-level FETI method. *Int. J. Numer. Methods Eng.*, 50:1523 – 1544, 2001.
3. C. Hofer. Analysis of discontinuous Galerkin dual-primal isogeometric tearing and interconnecting methods. *Math. Models Methods Appl. Sci.*, 28(1):131 – 158, 2018.
4. T. J. R. Hughes, J. A. Cottrell, and Y. Bazilevs. Isogeometric analysis: CAD, finite elements, NURBS, exact geometry and mesh refinement. *Comput. Methods Appl. Mech. Eng.*, 194(39-41):4135 – 4195, 2005.
5. S. Kleiss, C. Pechstein, B. Jüttler, and S. Tomar. IETI-Isogeometric Tearing and Interconnecting. *Comput. Methods Appl. Mech. Eng.*, 247-248:201 – 215, 2012.
6. J. Mandel, C. R. Dohrmann, and R. Tezaur. An algebraic theory for primal and dual substructuring methods by constraints. *Appl. Numer. Math.*, 54(2):167 – 193, 2005.
7. S. V. Nepomnyaschikh. Optimal multilevel extension operators. <https://www.tu-chemnitz.de/sfb393/Files/PDF/spc95-3.pdf>, 1995.
8. R. Schneckleitner and S. Takacs. Condition number bounds for IETI-DP methods that are explicit in h and p . *Math. Models Methods Appl. Sci.*, 30(11):2067 – 2103, 2020.
9. R. Schneckleitner and S. Takacs. Convergence theory for IETI-DP solvers for discontinuous Galerkin Isogeometric Analysis that is explicit in h and p . arXiv: 2005.09546 [math.NA], 2020.
10. A. Toselli and O. B. Widlund. *Domain Decomposition Methods – Algorithms and Theory*. Springer, Berlin, 2005.

Latest Reports in this series

2009 - 2018

[..]

2019

- | | | |
|---------|---|---------------|
| 2019-01 | Helmut Gfrerer and Jiří V. Outrata
<i>On a Semismooth* Newton Method for Solving Generalized Equations</i> | April 2019 |
| 2019-02 | Matúš Benko, Michal Červinka and Tim Hoheisel
<i>New Verifiable Sufficient Conditions for Metric Subregularity of Constraint Systems with Applications to Disjunctive Programs</i> | June 2019 |
| 2019-03 | Matúš Benko
<i>On Inner Calmness*, Generalized Calculus, and Derivatives of the Normal-cone Map</i> | October 2019 |
| 2019-04 | Rainer Schneckleitner and Stefan Takacs
<i>Condition number bounds for IETI-DP methods that are explicit in h and p</i> | December 2019 |
| 2019-05 | Clemens Hofreither, Ludwig Mitter and Hendrik Speleers
<i>Local multigrid solvers for adaptive Isogeometric Analysis in hierarchical spline spaces</i> | December 2019 |

2020

- | | | |
|---------|---|---------------|
| 2020-01 | Ioannis Touloupoulos
<i>Viscoplastic Models and Finite Element Schemes for the Hot Rolling Metal Process</i> | February 2020 |
| 2020-02 | Rainer Schneckleitner and Stefan Takacs
<i>Convergence Theory for IETI-DP Solvers for Discontinuous Galerkin Isogeometric Analysis That Is Explicit in h and p</i> | May 2020 |
| 2020-03 | Svetoslav Nakov and Ioannis Touloupoulos
<i>Convergence Estimates of Finite Elements for a Class of Quasilinear Elliptic Problems</i> | May 2020 |
| 2020-04 | Helmut Gfrerer, Jiří V. Outrata and Jan Valdman
<i>On the Application of the Semismooth* Newton Method to Variational Inequalities of the Second Kind</i> | July 2020 |

2021

- | | | |
|---------|--|---------------|
| 2020-01 | Ioannis Touloupoulos
<i>A Continuous Space-Time Finite Element Scheme for Quasilinear Parabolic Problems</i> | February 2021 |
| 2020-02 | Rainer Schneckleitner and Stefan Takacs
<i>Towards a IETI-DP Solver on Non-Matching Multi-Patch Domains</i> | March 2021 |
| 2020-03 | Rainer Schneckleitner and Stefan Takacs
<i>IETI-DP for Conforming Multi-Patch Isogeometric Analysis in Three Dimensions</i> | March 2021 |

From 1998 to 2008 reports were published by SFB013. Please see

<http://www.sfb013.uni-linz.ac.at/index.php?id=reports>

From 2004 on reports were also published by RICAM. Please see

<http://www.ricam.oeaw.ac.at/publications/>

For a complete list of NuMa reports see

<http://www.numa.uni-linz.ac.at/Publications/List/>